function sample the magnitude and even the sign of the polarization are different. This is due to those photoexcited electrons whose final-state energy lies between the vacuum levels of the two samples: only in case of the lower work function do they contribute to the photocurrent, thereby affecting the ESP. The interpretation of the magnitude of the polarization requires a quantitative comparison with calculated spectra and is not attempted in this paper.

From the two spectra, the five interband energies shown in Fig. 3 are derived: transition a_{6-7}, 3.6 (3.8); b_{5-7}, 4.8 (5.2); c_{4-7}, 5.8 (5.9); $d_{5,6-7}$, 6.9 (7.5); and e_{4-7}, 7.6 (8.6). All values are given in eV, with the theoretical ones in parentheses. The subscripts denote the bands involved in the transition.

A surprising feature of the clean spectrum is that the positive polarization is present right from the photothreshold although according to the band calculation the first interband transition along Λ should occur only at 7.5 eV. We attribute this to hole lifetime broadening: For the clean sample the initial-state energies lie at the top of the d-band density of states which is very large, resulting in short hole lifetime.

The spin-polarized photoemission experiments on gold exhibit the specific advantages of this method: (1) increased resolution, typical for a differential measurement as compared to an intensity measurement, and (2) unambiguous assignment of the bands due to the sign of the final-state polarization. Furthermore the restriction of polarization to transitions at lines or points of high symmetry selects automatically the most interesting parts of the Brillouin zone. The experiments show that optical orientation presents a powerful and, in certain cases, even unique tool for the investigation of the electronic structure of solids.

We thank H. C. Siegmann for his continuous encouragement and stimulating discussions. The financial support by the Schweizerische Nationalfonds is gratefully acknowledged.

[1]N. Egede Christensen and B. Seraphin, Phys. Rev. B 4, 3321 (1971), and Solid State Commun. 37, 57 (1981).

[2]P. Heimann, H. Miosga, and H. Neddermeyer, Solid State Commun. 29, 463 (1979); R. Mosei, R. Lässer, N. V. Smith, and R. L. Benbow, Solid State Commun. 35, 979 (1980).

[3]We thank J. R. Noonan, Oak Ridge National Laboratory, for giving details about the electropolishing procedure.

[4]S. F. Alvarado, W. Eib, F. Meier, H. C. Siegmann, and P. Zürcher, in *Photoemission from Surfaces*, edited by B. Feuerbacher and B. Fitton (Wiley, New York, 1978).

[5]M. Wöhlecke and G. Borstel, Phys. Rev. B 23, 980 (1981).

[6]The symmetry of the bands is characterized by a superscript for the single-group representation and a subscript for the double-group representation.

[7]W. J. Scouler, Phys. Rev. Lett. 18, 445 (1967).

Excitation Spectrum of the Ising-Heisenberg Chain Ferromagnet

T. Schneider and E. Stoll
IBM Zurich Research Laboratory, CH-8803 Rüschlikon-ZH, Switzerland
(Received 6 May 1981)

Results are presented and interpreted for the zero- and finite-temperature excitation spectrum of ferromagnetic Ising-Heisenberg chains, as probed by dynamic form factors. Finite-chain calculations demonstrate the occurrence of a thermally induced resonance centered around zero frequency, and a broadening of the magnon and two-magnon bound-state resonances at low T. The occurrence of bound states in the associated transitions demonstrates the failure of finite-order magnon perturbation theory.

PACS numbers: 75.10.Hk, 75.10.Jm

The quantum and classical properties of one-dimensional systems, including the thermodynamics, the dynamics, and soliton aspects are subjects of considerable renewed interest and activity.[1-3] Nevertheless, the development is hampered by lack of exact results for time-dependent correlation functions and the associated dynamic form factors, allowing unraveling of the excitation spectrum, as probed by dynamic form factors, at finite temperature.

© 1981 The American Physical Society

In this Letter, we present and unravel the excitation spectrum of finite spin-$\frac{1}{2}$ Ising-Heisenberg chains at finite T. The Hamiltonian is

$$\mathcal{H} = -J \sum_{j=1}^{N} [S_j^z S_{j+1}^z + g^{-1}(S_j^x S_{j+1}^x + S_j^y S_{j+1}^y)]. \quad (1)$$

Periodic boundary conditions are assumed, and g varies between the Ising limit $g=\infty$ and the isotropic Heisenberg model $g=1$.

The exact results for the stationary states and the eigenvalue spectrum[4-6] reveal that magnon and magnon bound states represent the elementary excitations of the system. Considerable progress has also been made regarding the thermodynamic properties.[7-9] Moreover, by using the equation-of-motion technique for Green's functions, certain dynamic form factors defined by

$$S_{AA}(q,\omega) = (1/Z) \sum_{\lambda,\lambda'} e^{-\beta\omega_\lambda} |\langle\lambda|A(q)|\lambda'\rangle|^2 \times \delta(\omega - \omega_{\lambda'} + \omega_\lambda) \quad (2)$$

can be evaluated exactly at $T=0$.[10] Here,

$$A(q) = (1/\sqrt{N}) \textstyle\sum_l A_l e^{iql}, \quad (3)$$

Z is the partition function, λ the stationary states with eigenvalue ω_λ, $\beta = 1/k_B T$, ω the frequency, and q the wave number.

We consider the operators

$$A_l = \begin{cases} S_l^x \\ S_l^+ S_{l+1}^+ \end{cases} \quad (4)$$

where

$$S_l^+ = S_l^x + iS_l^y. \quad (5)$$

The associated dynamic form factors will be labeled by $S_{xx}(q,\omega)$ and $S_{11}(q,\omega)$. Following Wortis,[10] these quantities can be calculated exactly at $T=0$, by using the equation of motion of the corresponding Green's function. We obtain

$$S_{xx}(q,\omega) = \tfrac{1}{4}\delta[\omega - \omega_1(q)], \quad (6)$$

where the magnon frequency is given by

$$\omega_1(q) = J(1 - g^{-1}\cos q). \quad (7)$$

Accordingly, the spectrum is exhausted by the elementary excitation, the magnon. For $S_{11}(q,\omega)$, describing the fluctuations of two adjacent spin deviations, we find

$$S_{11}(q,\omega) = [\omega_2(q)/J]\,\delta[\omega - \omega_2(q)] \quad (8)$$

for

$$\omega < \omega_{BC}(q) = 2J(1 - g^{-1}\cos q/2). \quad (9)$$

The two-magnon bound-state frequency is given by

$$\omega_2(q) = J(1 - g^{-2}\cos^2 q/2). \quad (10)$$

At and above $\omega_{BC}(q)$, the bottom of the two-magnon continuum, we find

$$S_{11}(q,\omega) = \frac{2}{\pi J}\left(\frac{\cos q/2}{g}\right)^2 \frac{B}{B^2 + [2(g^{-1}\cos q/2)^2 - 2 + \omega/J]^2}, \quad (11)$$

where

$$B = J^{-1}\{[\omega - \omega_{BC}(q)][\omega_{TC}(q) - \omega]\}^{1/2}, \quad (12)$$

$$\omega_{TC}(q) = 2J(1 + g^{-1}\cos q/2). \quad (13)$$

Thus, the spectrum of $S_{11}(q,\omega)$ exhibits a δ peak associated with the two-magnon bound state and a two-magnon continuum resonance bounded by the top $[\omega_{TC}(q)]$ and bottom $[\omega_{BC}(q)]$ of the continuum. The resulting dispersion curves are given in Fig. 1 for $g^{-1}=0.13$ and the Ising limit $g^{-1}=0$. In the latter case, the spectrum becomes particularly simple, because Eqs. (6), (8), and (11) reduce, for $g\to\infty$, to

$$S_{xx}(q,\omega) = \tfrac{1}{4}S_{11}(q,\omega) = \tfrac{1}{4}\delta(\omega - J), \quad (14)$$

so that the magnon and two-magnon bound state become degenerate, and the weight of the two-magnon continuum vanishes. For $g^{-1}=0$, this degeneracy extends to all multimagnon bound states.[6] For $q=0$, it also occurs in the Heisenberg limit ($g=1$), where according to Eqs. (7), (9), and (10) the gaps vanish, because $\omega_1(q=0) = \omega_{BC}(q=0) = \omega_2(q=0) = 0$. These $T=0$ results then reveal that $S_{xx}(q,\omega)$ probes the magnon, while $S_{11}(q,\omega)$ unravels the two-magnon bound state and the two-magnon continuum.

At finite temperatures, however, the problem becomes much more complicated because the states $\langle\lambda|$ with eigenvalue ω_λ, appearing in Eq. (2), no longer include the ground state only. Accordingly, transitions between excited states will give rise to additional contributions. To clarify the detailed origin of this thermally induced structure, we calculated $S_{xx}(q,\omega)$ and $S_{11}(q,\omega)$ numerically for finite chains subjected to periodic boundary conditions. Clearly, $S(q,\omega)$ will consist of discrete lines whose height is calculated on the basis of Eq. (2) by using the numerically evaluated eigenvalues and eigenfunctions of $\mathcal{H}$.[11-15] Comparison with the corresponding zero-tem-

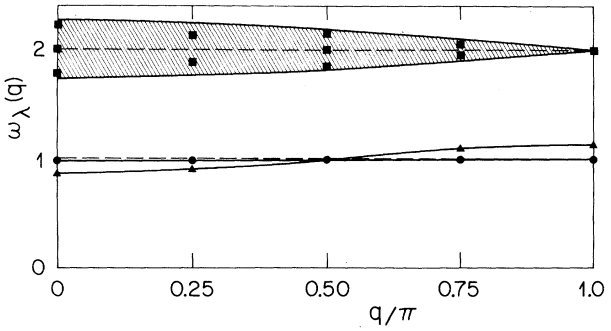

FIG. 1. Dispersion curves for $g^{-1}=0.13$. Solid line with triangles, magnons; solid line with circles, two-magnon bound state. The shaded area is the two-magnon continuum. The dashed line corresponds to the Ising limit $g=\infty$. Triangles, circles, and squares denote magnons, two-magnon bound states, and two-magnon continuum states, respectively, for $N=8$.

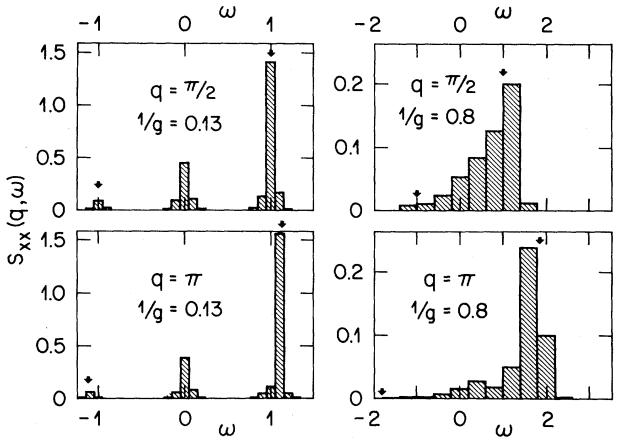

FIG. 2. $S_{xx}(q,\omega)$ for $N=8$, $T/J=\frac{1}{3}$, $q=\pi/2$ and π, with $g^{-1}=0.13$ and 0.8, respectively. The arrows mark the magnon frequencies [Eq. (7)].

perature results [Eqs. (6), (8), and (11)], indicates that $N=8$ reproduces the resonance structure of the infinite system sufficiently well to clarify its origin.

Figure 2 shows some results for $S_{xx}(q,\omega)$ at $T/J=\frac{1}{3}$, belonging to the low-T regime, where the spectra are still dominated by the resonance, corresponding at $T=0$ to the creation of a magnon [Eq.(6)]. Nevertheless, Fig. 2 clearly reveals considerable thermally induced structure. The "magnon" resonance adopts a finite width, and the corresponding destruction peak and a central peak (CP), clearly visible for $g^{-1}=0.13$, and $g^{-1}=0.8$ at $q=\pi$, appear. A detailed analysis of the contributions to $S_{xx}(q,\omega)$ [Eq. (2)] in terms of the eigenstates and eigenvalues reveals that the dominant thermally induced weight to the CP stems from difference processes between two- and three-magnon bound states, as well as between two-magnon bound states and magnons. Moreover, broadening of the magnon resonances involves transitions between the two-magnon bound states and the three-magnon continuum. These findings lead to the important conclusion that finite-order magnon perturbation theory cannot account for the thermally induced features, because they involve bound states, representing an infinite-order phenomenon.

Some results for $S_{11}(q,\omega)$ at $T=0$ and $T/J=\frac{1}{3}$ are shown in Fig. 3. Comparison with the exact $T=0$ results for $N=\infty$ clearly reveals that $N=8$ is sufficient to elucidate the physical origin of the resonances associated with an infinite system. For $g^{-1}=0.13$, and $T/J=\frac{1}{3}$ the spectra are dom-

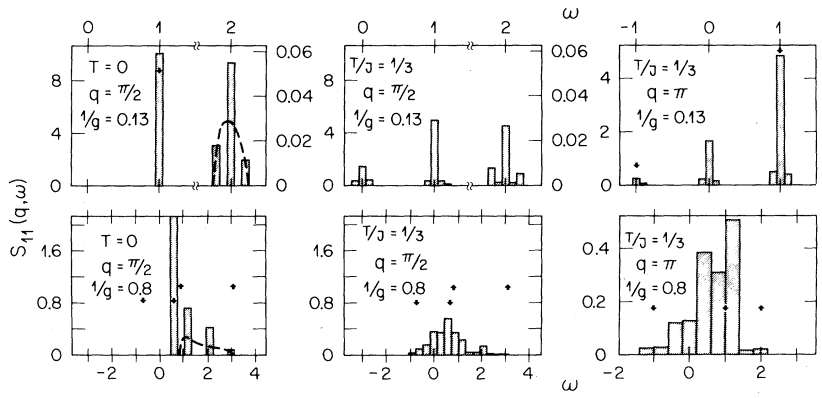

FIG. 3. $S_{11}(q,\omega)$ for $N=8$, $q=\pi/2$ and π, with $g^{-1}=0.13$ and 0.8, respectively. Downward-pointing arrows mark the bound-state frequencies [Eq. (10)], and upward ones the bottom and top of the continuum [Eqs. (9) and (13)] for $g^{-1}=0.8$. Dashed lines: two-magnon continuum resonance at $T=0$ and $N=\infty$ [Eq. (11)].

inated by the resonance, corresponding at $T=0$ to the creation of a bound state [Eq. (8)]. The thermally induced structure leads to a broadening of the two-magnon bound-state resonance, the corresponding destruction peak, and a CP. The dominant contributions to this CP can be traced back to difference processes between two-magnon and four-magnon bound states, as well as between magnons and three-magnon bound states. Broadening of the bound-state resonance is dominated by two-magnon bound state to magnon continuum and four-magnon bound state to magnon-continuum transitions. At $T=0$, $g^{-1}=0.8$, and $q=\pi/2$, the high-frequency tail of $S_{11}(q,\omega)$ is exhausted by the continuum contribution, which vanishes at $q=\pi$. This trend is still seen at $T/J=\frac{1}{3}$. The remaining structure and its interpretation is very similar to that at $g^{-1}=0.13$, with the important difference, however, that the resonances are much broader. This effect merely reflects the more pronounced dispersion close to the Heisenberg limit.

Calculations have also been performed for $T/J=\frac{2}{3}$ and 1, revealing that in both $S_{xx}(q,\omega)$ and $S_{11}(q,\omega)$, the CP grows faster than the magnon, two-magnon bound state, and continuum resonances with increasing temperature.

Summarizing, we have shown that the excitation spectrum of the Ising-Heisenberg ferromagnet becomes dramatically modified at finite temperature. The most striking new feature is a resonance centered around zero frequency in $S_{xx}(q,\pi)$ and $S_{11}(q,\pi)$, associated with difference processes between bound states, as well as between magnons and bound states. This CP grows faster than the remaining structure with increasing temperature. Moreover, the thermally induced broadening of the magnon and the two-magnon bound-state resonances was found to involve bound states, too. Consequently, these results clearly demonstrate the failure of finite-order magnon perturbation theory. The Ising-like ferromagnetic chains $CoCl_2\cdot 2H_2O$ [16] and $CoCl_2\cdot 2NC_5H_5$ and the recent discovery of a family of spin-$\frac{1}{2}$ Heisenberg chains[17] offer the possibility of observing these thermally induced phenomena experimentally.

We note that $S_{xx}(q,\omega)$ is related to the neutron-scattering cross section, and $S_{11}(q,\omega)$ might be probed by light-scattering techniques.[16]

Finally, we note that our results, strictly valid for $s=\frac{1}{2}$ only, remain qualitatively correct for larger s values. In fact, the main physical content of Eqs. (6), (8), and (11), predicting magnon, two-magnon bound state, and continuum resonances, simply follows from the classification of the states according to the eigenvalues of the spin deviation operator, $n=Ns+\sum_l S_l^z$. Consequently, even the finite-T behavior will involve the same transitions, giving rise to a thermally induced structure, similar to that outlined above for $s=\frac{1}{2}$. In this view, the classical limit of our results will also clarify the relevance of the envelope solitons associated with the classical continuum version of the Ising-Heisenberg model.[18]

[1]J. C. Bonner, J. Appl. Phys. 49, 1299 (1978).

[2]*Solitons and Condensed-Matter Physics*, edited by A. R. Bishop and T. Schneider (Springer, Heidelberg, 1978).

[3]*Physics in One Dimension*, edited by J. Bernasconi and T. Schneider (Springer, Heidelberg, 1981).

[4]H. A. Bethe, Z. Phys. 71, 205 (1931).

[5]R. Orbach, Phys. Rev. 112, 309 (1958).

[6]I. G. Gochev, Zh. Eksp. Teor. Fiz. 61, 1674 (1972) [Sov. Phys. JETP 34, 892 (1972)].

[7]J. C. Bonner and M. E. Fisher, Phys. Rev. 135, A540 (1964).

[8]M. Gaudin, Phys. Rev. Lett. 26, 1301 (1971).

[9]J. D. Johnson and J. C. Bonner, Phys. Rev. Lett. 44, 616 (1980), and Phys. Rev. B 22, 251 (1980).

[10]M. Wortis, Phys. Rev. 132, 85 (1963).

[11]F. Carboni and P. M. Richards, Phys. Rev. 177, 889 (1969).

[12]G. Müller and H. Beck, J. Phys. C 11, 483 (1978).

[13]G. Müller, H. Beck, and J. C. Bonner, Phys. Rev. Lett. 43, 75 (1979).

[14]J. P. Groen, T. O. Klaassen, N. J. Paulis, G. Müller, H. Thomas, and H. Beck, Phys. Rev. B 22, 5369 (1980).

[15]N. Ishimura and H. Shiba, Prog. Theor. Phys. 63, 743 (1980).

[16]J. B. Torrance, Jr., and M. Tinkham, Phys. Rev. 187, 595 (1969).

[17]C. P. Landee and R. D. Willett, Phys. Rev. Lett. 43, 463 (1979).

[18]E. K. Sklyanin, to be published.